ECS Journal of Solid State Science and Technology, **7** (5) P281-P286 (2018)
2162-8769/2018/7(5)/P281/6/$37.00 © The Electrochemical Society

Interfacial Chemistry Study of GaN by Trimethylaluminum-Only Cycles and X-ray Photoelectron Spectroscopy

T. L. Duan,[1,z] J. S. Pan,[2] D. S. Ang,[3] and C. J. Gu[4]

[1]*Materials Characterization and Preparation Center, Southern University of Science and Technology, Shenzhen, Guangdong 518055, China*
[2]*Institute of Materials Research and Engineering, A*STAR (Agency for Science, Technology and Research), Singapore 138634*
[3]*School of Electrical and Electronic Engineering, Nanyang Technological University, Singapore 639798*
[4]*Department of Microelectronics, Faculty of Science, Ningbo University, Ningbo 315211, China*

The interfacial chemistry of n-type Ga-face GaN during atomic layer deposition of Al_2O_3 is studied by preceding the deposition process with several trimethylaluminum(TMA)-only cycles to clarify the impact of this precursor on the Al_2O_3/GaN interface. X-ray photoelectron spectroscopy analysis shows that the TMA precursor can react with the surface gallium oxide (GaO_x) and convert the latter into aluminum oxide (AlO_x), in accordance to past reports. However, the extent of conversion is limited as the reaction between TMA and GaO_x is saturated after the first few TMA-only cycles. On the other hand, we found that the Ga/N ratio (GaN stoichiometry) is increased with the number of TMA-only cycles. At the same time, the Al-N bond peak appears in the Al 2*p* core-level spectrum, and its intensity also increases with the number of TMA-only cycles. The latter points to the formation of an Al-N layer, which may be attributed to Al ions from the TMA metal precursor penetrating the AlO_x/GaO_x layer and reacting with the underlying GaN. The reaction results in a loss of N from Ga bonding sites, and the increase of the Ga/N ratio. The resultant AlN layer protects the underlying GaN from oxidation and forms a high-quality interface with the Al_2O_3.
 [DOI: 10.1149/2.0251805jss]

Manuscript submitted March 14, 2018; revised manuscript received April 17, 2018. Published May 18, 2018.

GaN based high electron mobility transistor (HEMT) has found a broad application in high-frequency, high-power and high-temperature devices.[1–4] However, the high density of surface states that result from the native gallium oxide (GaO_x) is one of the critical issues in the development of the GaN HEMT technology.[5–7] Surface states give rise to a higher leakage current, lower breakdown field, and an unstable threshold voltage. To reduce the density of surface states, an insulator layer is inserted between GaN and the metal gate.[8] Besides serving as the gate dielectric and reducing the gate leakage of the metal-insulator-semiconductor HEMT (MIS-HEMT),[9] it is believed that the insulator also passivates the surface states. Among the various insulator materials examined, Al_2O_3 is preferred because it has a large bandgap (E_g ~7–9 eV), high dielectric constant (ε_r ~9) and high breakdown field (E_{bd} ~10 MV/cm).[10–12] The atomic layer deposition (ALD) process is commonly favored for the growth of Al_2O_3 as it provides excellent thickness control and a resultant high quality, conformal and uniform thin film.

The interface region between GaN and ALD Al_2O_3 has been studied intensively, both electrically and physically, in recent years.[11,13–15] Studies have suggested that the trimethylaluminum (TMA) metal precursor could remove the defective GaO_x and yield a high quality Al_2O_3/GaN interface.[11,12,16] However, the chemistry that takes place at the GaN surface during the ALD process and the nature of the resultant interfacial layer formed between Al_2O_3 and GaN have not been investigated in-depth. In this paper, we explore in detail the interfacial chemistry of GaN during Al_2O_3 deposition, using TMA-only cycles to clearly delineate the role of the metal precursor and a series of X-ray photoelectron spectroscopy (XPS) measurements to determine the electronic properties of GaN surface regions subjected to different experimental conditions. Although the results show that the TMA metal precursor could remove the GaO_x,[17,18] the effect is limited and is saturated after a few rounds of exposing the GaN surface to the precursor. More importantly, we found a non-negligible Al-N bond signal, whose intensity increases with the number of TMA-only cycles applied. As a thin AlN layer can protect the underlying GaN from oxidation,[7] the observed AlN formation thus provides another probable reason for the improved GaN and ALD Al_2O_3 interface.

A GaN-on-Si(111) wafer purchased from a commercial company was used in our study. The wafer surface has Miller indexes [0001] and it is a Ga-face wafer. The Ga-face wafer has smooth surface morphology and high material quality,[19] making it a preferred choice for device applications. A 1 μm Si-doped GaN layer sits on top of a 0.2 μm intrinsic GaN expitaxial layer, which is connected to the underlying Si substrate by a transitional buffer layer. The wafers were degreased in acetone and then in isopropyl alcohol for 5 minutes each. They were then dipped in dilute hydrofluoric acid ($HF:H_2O$ = 1:20) for ~3 minutes to remove the pre-existing native oxide and subsequently rinsed in flowing de-ionized water.

Three groups of samples (group A, B and C) were prepared and each group comprised four samples (each of dimensions 1 cm by 1 cm). All the samples were from the same wafer. Native GaO_x can regrow after the HF etch but the surface coverage is likely to be unsatisfactory within the experimental timeframe. To avoid ambiguity related to the incomplete native oxide regrowth after HF etch, both group A and B samples were subjected to O_2 annealing at a temperature of 500°C for 60 s in an AS-ONE RTP System, whereas this step was omitted for the group C samples (which serve as a reference). The resultant thermally grown GaO_x layer in the group A and B samples should have a more complete surface coverage as compared to the native counterpart in the group C samples. A past study on high-pressure oxidation of n-GaN epilayer has revealed a slow rate of ~0.3 nm/min at a temperature of 750°C.[20] Thus, we anticipate that the annealing conditions used in this study would only yield only several monolayers of thermal GaO_x in group A and B samples.

Group A samples A1-A4 each received 0, 1, 4, and 10 TMA-only cycles, respectively before the deposition of a ~3 nm Al_2O_3 layer. The Al_2O_3 deposition was carried out using alternating TMA and H_2O-vapor cycles. To distinguish the role of the TMA metal precursor during the Al_2O_3 deposition step, group B samples B1-B4 were each subjected to 0, 1, 4, 10 TMA-only cycles, respectively without subsequent Al_2O_3 deposition. A further reason for the omission of the Al_2O_3 deposition step will be clarified in a later discussion. Group C samples C1-C4 each received 1, 4, 10, 50 TMA-only cycles, respectively. No subsequent Al_2O_3 deposition was also carried out on this group of samples. For all the samples, the ALD chamber temperature was kept at 300°C. The experimental steps each sample underwent are given in Tables I, II and III for group A, B and C samples, respectively.

XPS measurements were carried out in a Thermo Fisher Scientific Theta Probe system equipped with a monochromatic, microfocused Al Kα (1486.6 eV) X-ray source and a hemispherical electron energy analyzer. The pass energy of the analyzer was set to 150 eV for the survey spectra and 40 eV for the individual core-level spectra. With this set-up, the full width at half maximum (FWHM) of the

[z]E-mail: duantl@sutstc.edu.cn

Table I. Binding energies of Ga 3*d*, N 1*s*, and Al 2*p* core-level spectra for samples A1-A4. Also shown are the ratio of the area under the Ga–O bond spectrum to the area under the Ga–N bond spectrum, and the ratio of the area under the Ga 3*d* spectrum (for Ga-N bond) to the area under the N 1*s* spectrum.

N-type Ga-face GaN wafer					Core-Level Binding Energy (eV)					Ratio	
					Ga 3*d*		N 1*s*	Al 2*p*			
Sample	Step 1	Step 2	Step 3 TMA-only cycle number	Step 4	Ga-N	Ga-O	Ga(Al)-N	Al-O	Al-N	Ga-O/Ga-N	Ga/N
A1	Acetone + IPA cleaning	RTA @ 500°C, 60 s in O_2	0	Al_2O_3 deposition ~3 nm	19.5	20.4	397.2	74.4	73.9	0.17	2.1
A2			1		19.6	20.5	397.2	74.4	73.8	0.17	2.1
A3			4		19.6	20.5	397.2	74.4	73.9	0.15	2.5
A4			10		19.7	20.5	397.4	74.5	73.7	0.21	3.1

Table II. Binding energies of Ga 3*d*, N 1*s*, and Al 2*p* the core-level spectra for samples B1-B4. The respective Ga–O to Ga–N bond ratio and Ga to N atomic ratio are also shown.

N-type Ga-face GaN wafer				Core-Level Binding Energy (eV)					Ratio	
				Ga 3*d*		N 1*s*	Al 2*p*			
Sample	Step 1	Step 2	Step 3 TMA-only cycle number	Ga-N	Ga-O	Ga(Al)-N	Al-O	Al-N	Ga-O/Ga-N	Ga/N
B1	Acetone+ IPA cleaning	RTA @ 500°C, 60 s in O_2	0	19.5	20.3	397.2	/-	/-	0.25	1.5
B2			1	19.6	20.5	397.2	74.5	73.9	0.2	1.7
B3			4	19.7	20.5	397.3	74.5	74.0	0.22	1.8
B4			10	19.7	20.6	397.4	74.7	74.2	0.22	1.9

Table III. Binding energies of Ga 3*d*, N 1*s*, and Al 2*p* core-level spectra for samples C1-C4. Also shown are the respective Ga–O to Ga–N bond ratio and Ga to N atomic ratio.

N-type Ga-face GaN wafer			Core-Level Binding Energy (eV)					Ratio	
			Ga 3*d*		N 1*s*	Al 2*p*			
Sample	Step 1	Step 2 TMA-only cycle number	Ga-N	Ga-O	Ga(Al)-N	Al-O	Al-N	Ga-O/Ga-N	Ga/N
C1	Acetone + IPA cleaning	1	19.5	20.3	397.1	74.6	73.9	0.15	1.5
C2		4	19.6	20.4	397.1	74.9	74.1	0.13	1.6
C3		10	19.4	20.2	397.1	74.7	74.1	0.13	1.6
C4		50	19.5	20.3	397.2	74.9	74.1	0.12	1.7

Ag $3d_{5/2}$ photoelectron peak was 0.5 eV. The XPS spectra were recorded at a detection angle (θ) of 60° with respect to the sample surface. The spectra were curve-fitted using the Avantage software, provided by the equipment manufacturer. Each component spectrum was represented by a combination of Gaussian (70%) and Lorentzian (30%) line shapes. The secondary electron background was subtracted utilizing the Shirley function. The FWHM of a given component spectrum was allowed to vary within a narrow range only (±0.1 eV). The lowest number of component spectra was used to obtain acceptably low residual values. Quantitative analysis, including element/bond ratio determination, was achieved using relative sensitivity factors and algorithms embedded in the Avantage software.[5] The binding energy (BE) calibration was performed using pure Ni, Au, Ag and Cu standard samples by setting the Ni Fermi edge, Au $4f_{7/2}$, Ag $3d_{5/2}$ and Cu $2p_{3/2}$ peaks at 0.00 ± 0.02 eV, 83.98 ± 0.02 eV, 368.26 ± 0.02 eV and 932.67 ± 0.02 eV, respectively. To eliminate any positive charge induced binding energy shift, besides a low energy electron flood gun was used for charge compensation during spectrum acquisition, the XPS spectra reported here are referenced to C 1s at 285.0 eV. The estimated uncertainty in the BE for a spectrum peak was at most ± 0.2 eV based on repeated measurements.

The Ga 3*d* core-level spectra for group A samples A1-A4 are shown in Fig. 1a. For each sample, the Ga 3*d* spectrum can be well fitted by the component peaks of the Ga-N and Ga-O bonds.[15,21] The Ga-O bond peak is due to GaO_x formation during the O_2 annealing step. The ratio of the Ga-O to Ga-N bond for each sample is given in Table I. This ratio is obtained by comparing the areas under the Ga-O and Ga-N spectra. It is noted that this ratio remains approximately constant for A1-A3 and is slightly increased for A4. Moreover, it is observed that the BE of the Ga-N bond is shifted to higher values when the number of the TMA-only cycles is increased. The Ga/N ratio (GaN stoichiometry) obtained by comparing the areas under the Ga 3*d* (Ga-N bond) and N 1*s* spectra (with atomic sensitivity factor correction included)[22] is also given in Table I. The Ga/N ratio can be seen to increase with the number of TMA-only cycles. This interestingly shows that the surface region of the GaN layer became slightly richer in Ga content after the TMA-only cycles. The N 1*s* core-level spectra for A1-A4 are given in Fig. 1b. One of the component peaks is labelled as Ga(Al)-N (open circles), instead of the usual Ga-N shown in past studies. The reason is that analysis of the Al 2*p* spectrum has shown the presence of a non-negligible Al-N component peak (see Figs. 1c, 2c and 3c).[15,21] Because the N 1*s* BE of Ga-N and Al-N bonds are almost the same, it is difficult to resolve these two bonds peaks in the N 1*s* core level spectrum. Therefore, the label of Ga(Al)-N attributes the peak to a combination of both Ga-N and Al-N bonds. Relative to A1, the BE for the Ga(Al)-N bond peak of A4 is increased by about 0.2 eV, similar to the increment seen in the Ga 3*d* BE in Fig. 1a. The Al 2*p* spectra for all the samples are given in Fig. 1c. Each spectrum may be fitted by the spectra of the Al-O and Al-N bonds. The observation of the Al-N bond signal should be emphasized as it suggests the formation of an AlN layer. However, the more dominant Al-O bond peak (as expected from the intentionally deposited Al_2O_3) may influence the

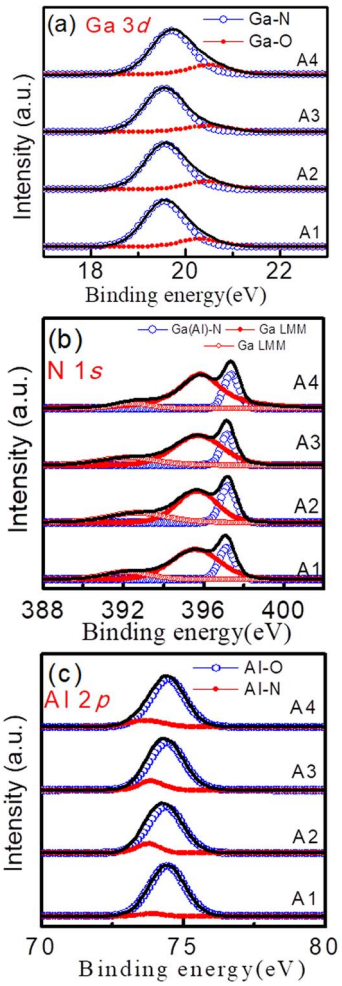

Figure 1. (a) Ga 3*d*, (b) N 1*s* and (c) Al 2*p* XPS core-level spectra for samples A1-A4.

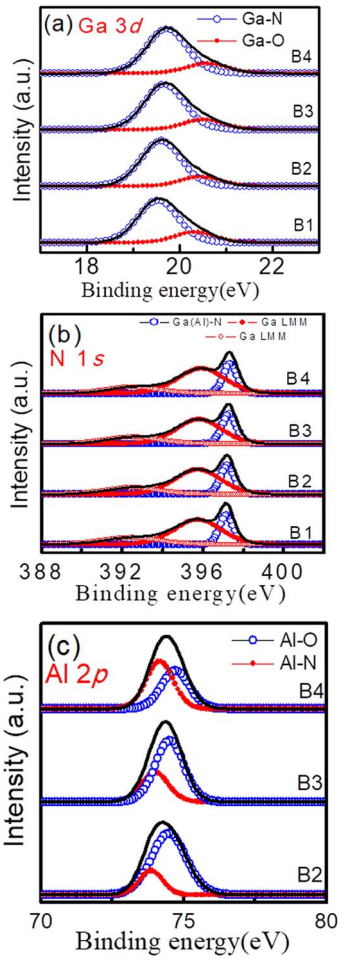

Figure 2. (a) Ga 3*d*, (b) N 1*s* and (c) Al 2*p* XPS core-level spectra for samples B1-B4.

accuracy of the Al-N bond peak fitting. Hence, group B samples are designed to validate the observation of Al-N formation and quantify its relationship with the number of TMA-only cycles.

For group B samples B1-B4, the Al_2O_3 deposition step was skipped and therefore changes in the XPS data are directly linked to the TMA-only cycles. The Ga 3*d* core-level spectra for B1-B4 are shown in Fig. 2a and are also well fitted by the spectra of the Ga-N and Ga-O bonds. The Ga-O/Ga-N ratio sees a slight decrease from B1 to B2 (which received 0 and 1 TMA-only cycle, respectively). However, for B3 and B4, which were subjected to increasingly more TMA-only cycles, this ratio is almost the same as that of B2. The initial decrease signifies that part of the GaO_x is converted to AlO_x by the TMA metal precursors.[18] The lack of a subsequent further decrease, when the number of TMA-only cycles is increased, indicates that the conversion has slowed down after the first few cycles. The absence of an initial decrease of this ratio in the group A samples may be ascribed to further GaN oxidation during the first few cycles of Al_2O_3 deposition, when the oxidizing agent was introduced.[16] This could in turn offset the decrease that arises from the TMA-only cycles, leading to an increase in some cases (A4). As compared to group A samples, the Ga-O/Ga-N ratios of group B samples are slightly larger. This may be because in the group A samples, the deposited Al_2O_3 layer helps protect the GaN surface from re-oxidation during subsequent ambient exposure. For B4, which was subjected to 10 TMA-only cycles, the BE of the Ga-N bond peak is increased by ~0.2 eV, relative to that of B1 (not exposed to any TMA-only cycle), similar to the trend seen in the group A samples. This shows that the TMA-only cycles play a key role in the observed shift in BE of the Ga-N bond peak; the subsequent Al_2O_3 deposition in the case of the group A samples has relatively less impact. It is also noticed that Ga/N ratio becomes larger with the increase of the number of TMA-only cycles, similar to the group A samples. However, the ratios for B1-B4 are smaller than the corresponding ratios of A1-A4 (see later explanation). The N 1*s* core-level spectra for B1-B4 are given in Fig. 2b. In going from B1 to B4, an overall increase in BE of the Ga(Al)-N bond peak by about 0.2 eV is also observed, in agreement with the observations from the Ga 3*d* spectra as well as the N 1*s* spectra of A1-A4 (cf. Fig. 1b). The Al 2*p* spectra, fitted by the spectra of the Al-O and Al-N bonds, are given in Fig. 2c. Presence of the Al-O bond spectrum, in the absence of Al_2O_3 deposition, confirms the formation of AlO_x due to the reaction between TMA and GaO_x.[18] Consistent observation of the Al-N signal for this group of samples validates the earlier inference that Al-N bonds were formed during the TMA-only cycles. This would likely involve Al ions from the TMA metal precursor penetrating the AlO_x/GaO_x layers and reacting with the underlying GaN surface. The Al-N peak intensity can be seen to increase with the number of TMA-only cycles. In fact, B4 shows a higher Al-N bond peak than the Al-O bond peak, indicating the gradual dominance of Al-N bond formation as the number of TMA-only cycles is increased. With a longer cumulative exposure to the TMA metal precursor, more of the Al ions could penetrate the AlO_x/GaO_x layer and react with the underlying GaN to form Al-N bonds. The core-level BEs, Ga-O/Ga-N and Ga/N ratios pertaining to B1-B4 are summarized in Table II.

To check the influence of the native GaO_x layer on the interfacial chemistry of GaN during the ALD process, group C samples C1-C4,

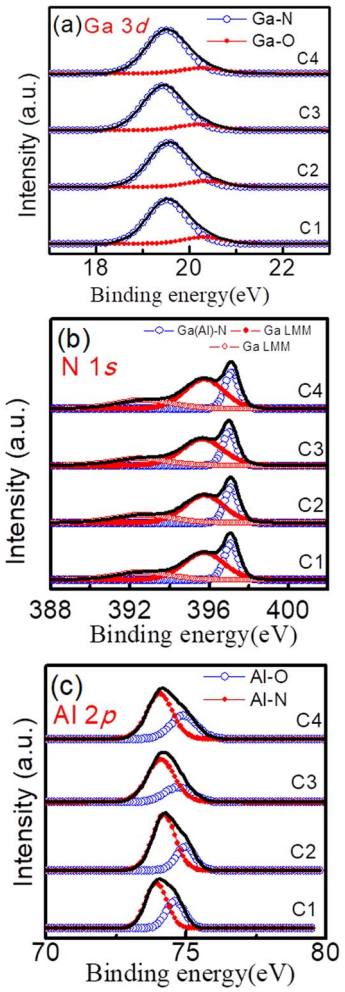

Figure 3. (a) Ga 3*d*, (b) N 1*s* and (c) Al 2*p* XPS core-level spectra for samples C1-C4.

which did not undergo the O_2 annealing step, were prepared. The Ga 3*d* core-level spectra, fitted with the spectra of the Ga-N and Ga-O bonds, are shown in Fig. 3a. Similar to the group B samples, the Ga-O/Ga-N ratio shows a slight decrease initially and then it stays relatively constant thereafter, even after 50 TMA-only cycles (C4). Because C1-C4 did not undergo the O_2 annealing step, the Ga-O/Ga-N ratios are the lowest for the group C samples. Unlike the group A and B samples (which registered a 0.2 eV increase of the Ga-N bond peak after 10 TMA-only cycles), the BE of the Ga-N bond peak in group C samples is unaffected by the number of TMA-only cycles (even after 50 such cycles). It should be noted that the similar 0.2 eV BE shift of the Ga-N bond peak of group A and B samples has helped to rule out the role of Al_2O_3 deposition on the observed BE shift in the former. The most distinct difference among these three groups of samples is the type of GaO_x (thermally grown GaO_x for group A and B and native oxide for group C). Thus, this is a probable cause for the discrepancy in the Ga-N bond peak BE results mentioned above (a possible explanation is given later). As for the Ga/N ratio, a gradual increase with the number of TMA-only cycles is evident, just like those of the group A and B samples. The N 1*s* core-level spectra for C1-C4 are given in Fig. 3b; here the BE for the Ga(Al)-N bond peak is also not affected by the number of TMA-only cycles, in agreement with the observation made on the Ga 3*d* spectra. The Al 2*p* core-level spectra are given in Fig. 3c. It is noted that the Al-N bond peak is larger than the Al-O bond peak in all the samples. This observation should be compared against that of the group B samples (B2 and B3), which show a smaller Al-N bond peak when only a couple of TMA-only cycles are applied. The more dominant Al-N bond peak in group C samples may be attributed to the poorer surface coverage of the native GaO_x layer, which allows a more direct interaction between the TMA metal precursor and the GaN, leading to more Al-N bond formation. Table III summarizes the core-level BEs and Ga-O/Ga-N and Ga/N ratios of C1-C4.

From the XPS data presented above, we summarize two key findings as follows:

First, the appearance of an Al-O bond signal upon the application of a TMA-only cycle (B2) and the decrease of the GaO-to-GaN ratio of group B and C samples when the TMA-only cycles were first applied indicate that GaO_x is being converted to AlO_x, in accordance to past studies.[18] The conversion has generally been explained in terms of the more negative Gibb's free energy of Al_2O_3 (−1582 kJ/mol), as compared to that of Ga_2O_3 (−998 kJ/mol).[16,23] Hence, the formation of Al_2O_3 is preferred over Ga_2O_3, under a given set of conditions. However, the marginal decrease in the Ga-O/Ga-N ratio and the lack of any further decrease after more TMA-only cycles are applied indicate that complete removal of GaO_x by the TMA precursors is unlikely to happen under typical ALD process which involves oxidant cycles that would induce further oxidation of the GaN surface in the initial stage.[16] The results imply that the interaction between the TMA precursor and GaO_x occurs at the latter's surface, with the Al-O bond formation facilitated by the dangling O bonds there. Fig. 4a schematically depicts this surface reaction on a partially ordered GaO_x layer formed after thermal oxidation.[6,15] Once all available reaction sites are used up, the conversion slows down. The conversion of the remaining GaO_x into Al_2O_3 may presumably involve other energy barriers and is less favorable than that suggested by the Gibb's free energy difference. This subject is under further study.

Second, the observation of an Al-N bond signal, whose intensity grows with the number of TMA-only cycles, points to a reaction between Al ions from the TMA metal precursor and the underlying GaN region. This should involve the penetration of Al ions through the native or thermally grown GaO_x layer and their subsequent reaction with the underlying GaN region, as depicted schematically in Fig. 4b. Past studies have shown that Al could attract N from GaN,[24–26] consistent with our observation of Al-N formation in this study. The GaN to AlN conversion occurs because AlN has more negative Gibb's free energy (−287.4 kJ/mol) than that of GaN (−98.7 kJ/mol).[23,27,28] It has also been reported that a thin AlN layer formed on GaN could protect the latter from oxidation.[7,14] Hence, the observed formation of Al-N in this study should serve as an additional consideration behind the improved GaN surface quality after Al_2O_3 deposition, besides conversion of GaO_x to AlO_x. The reaction between Al and N depletes the latter from the Ga bonding sites and generate N vacancy defects in the GaN surface region (Fig. 4). The corresponding increase of the Ga/N ratio, which indicates that the GaN surface region becomes gradually richer in Ga content as more TMA-only cycles are applied, corroborates the observation of Al-N formation.

Next, we turn the attention to the Ga-N bond peak BE shift seen for group A and B samples after exposure to the TMA metal precursor, and the lack of such a shift in group C samples. Studies have indicated that the disordered native GaO_x give rise to donor-like surface states, i.e. positively charged when situated above the Fermi level.[29] Therefore, these donor-like states could negate the negative surface charge arising from the spontaneous polarization effect and reduce the upward energy band bending at the n-type GaN surface.[30,31] Annealing in an O_2 ambient reduces the density of these defect states, due to the formation of an ordered thermal GaO_x layer.[6,15] A thin GaO_x layer formed before Al_2O_3 deposition is found to passivate the surface states effectively.[15]

We have earlier found that the extracted BE of the Ga-N and Ga-O bond peaks are affected by the upward surface band bending and the probe depth of XPS.[5] Any change in BE may therefore be related to possible changes in the net surface charge and XPS probe depth. In A1-A4, a 3-nm think Al_2O_3 layer was deposited after the TMA-only cycles. Thus, the XPS probe depth of GaN layer in these samples should be shallower than that in the group B samples, as shown in

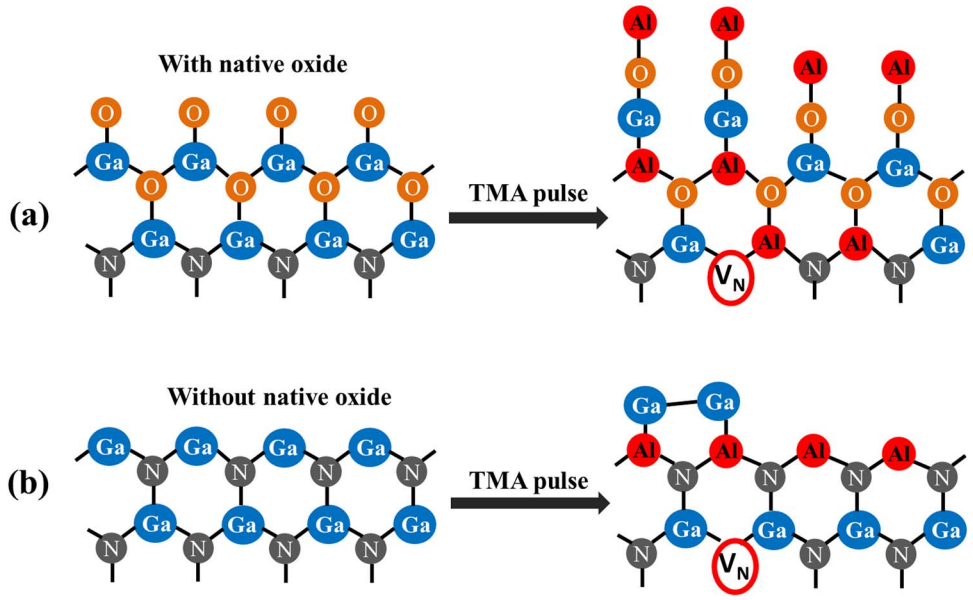

Figure 4. Schematic of the TMA metal precursor interaction with GaN for the case (a) with and (b) without a surface gallium oxide layer. Since Al ions draw N ions from underlying GaN to form the AlN layer, this results in the generation of N vacancies (V_N's) and thus the GaN surface becomes Ga-rich.

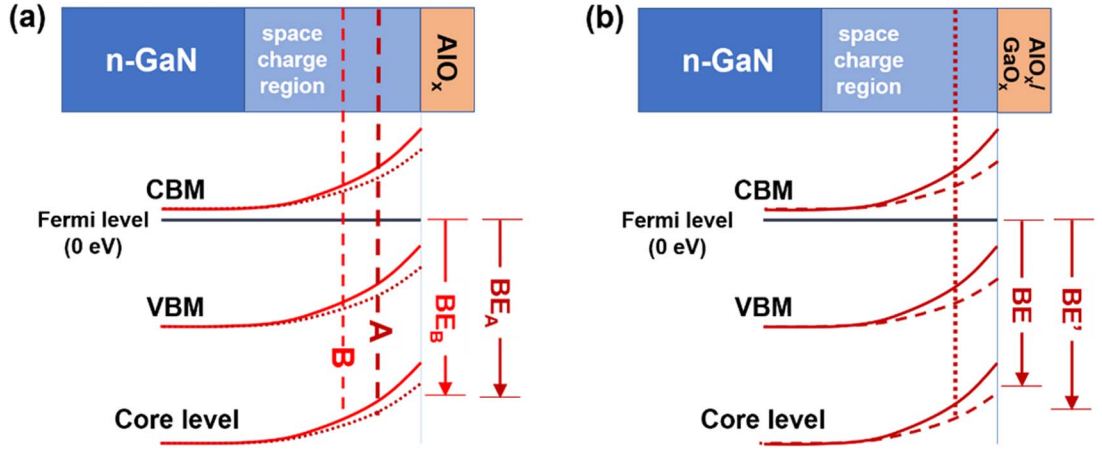

Figure 5. Schematic energy band diagrams of the depleted n-GaN surface region due to negative surface polarization charge, showing the dependence of the measured core-level binding energy (BE) on changes in the XPS probe depth and/or surface band bending. (a) The decrease in BE in a group A sample due to the shallower XPS probe depth in the GaN region (relative to that in a group B sample) is offset by the reduced surface band bending (dotted lines) arising from positive charges in the Al_2O_3. (b) An increase in positive surface charge reduces the upward band bending (dashed lines), leading to an increase in the measured core-level BE. CBM and VBM denote the conduction band minimum and valence band maximum, respectively.

Fig. 5a. However, the core-level BEs for both group of samples are comparable. This may be explained by the higher positive charge density in group A samples arising from the deposited Al_2O_3 layer.[16] Hence, the net surface charge density is less negative in this group of samples than that in the group B samples. The resultant smaller upward band bending in the former compensates the decrease expected from the shallower XPS probe depth.

Since group A and B samples are subjected to an O_2 annealing step, the surface state density is reduced by the thermally grown GaO_x.[15] However, the conversion of the thermal GaO_x into AlO_x by the TMA metal precursor would disrupt the ordered structure of the thermal oxide, increasing the density of the positively charged surface states. It has also been reported that N vacancies in the GaN surface region give rise to donor-like defective states.[32] As a result, the net surface charge becomes less negative and the upward surface band bending reduced, which in turn leads to an increase in the measured BE of the Ga-N and Ga-O bond peaks (Fig. 5b). On the other hand, the native GaO_x layer in group C samples is already in a disordered state and the subsequent conversion to AlO_x would have a relatively less impact on its structure, and in turn on the net surface charge density. This explains the lack of any apparent shift in the core-level BEs.

Difference in the Ga/N ratio of the three groups of samples, highest for group A, intermediate for group B and lowest for group C, could also be consistently explained. It has been reported that an O_2 annealing step would decompose the structure of the GaN surface region and result in a Ga-rich surface.[5] This explains the higher Ga/N ratio of group B samples (subjected to the O_2 annealing step), as compared to that of group C (which did not undergo the O_2 annealing step). In group A samples, the deposition of a 3-nm thick Al_2O_3 followed the TMA-only cycles. The deposition rate for the conditions used in this study is ~0.9 nm/cycle. Hence, group A samples were subjected to more than 30 more TMA cycles than the other two group of samples. Penetration of Al ions from the TMA metal precursor and reaction with the underlying GaN in these additional TMA cycles involved in the Al_2O_3 deposition may contribute to the higher Ga/N ratio in the group A samples. Furthermore, since the XPS probe depth in the

GaN layer of group A sample is nearer to the GaN/oxide interface in comparison to group B and C samples, this may also be a reason for the higher Ga/N ratio in the group A samples.

In this study, the influence of TMA cycles on the interfacial chemistry of GaN during Al_2O_3 deposition is clarified through TMA-only cycles applied before the Al_2O_3 deposition step, to understand the reason for the good Al_2O_3/GaN interface quality reported in the literature. Although a decrease in the Ga-O/Ga-N bond ratio is observed, suggesting that the native or thermally grown GaO_x is converted into AlO_x,[18] the decrease of the ratio only occurs for the initial few TMA-only cycles, and it remains unchanged for a further increase of the TMA-only cycles. This shows that the GaO_x to AlO_x conversion effect is limited by the saturation that sets in after the initial TMA cycles. Moreover, in a typical ALD process which involves the alternate application of TMA and oxidant cycles, an increase of the GaO/GaN ratio has been observed due to the oxidation of the underlying GaN region.[16] Besides the abovementioned, XPS measurements also reveal the presence of the Al 2*p* core-level spectrum associated with the Al-N bond, and the enhancement of the bond peak intensity with the number of applied TMA-only cycles. This points to the formation of an Al-N layer, due to the Al ions from the TMA metal precursor reacting with the underlying GaN during the ALD process. This study shows the formation of AlN as another probable reason for the commonly observed improvement of GaN surface quality after Al_2O_3 deposition. However, the increase in N vacancies may be a concern and is a tradeoff that would probably have to be addressed through other means (e.g. by intentionally increasing the surface N content before Al_2O_3 deposition) and is a subject for further study.

ORCID

T. L. Duan https://orcid.org/0000-0001-5165-4141
C. J. Gu https://orcid.org/0000-0002-1339-4534

References

1. F. M. Barradas, L. C. Nunes, T. R. Cunha, P. M. Lavrador, P. M. Cabral, and J. C. Pedro, *IEEE Transactions on Microwave Theory and Techniques*, **65**, 3379 (2017).
2. P. Fiorenza, G. Greco, F. Iucolano, A. Patti, and F. Roccaforte, *IEEE Trans. Electron Devices*, **64**, 2893 (2017).
3. A. Mojab, Z. Hemmat, H. Riazmontazer, and A. Rahnamaee, *IEEE Trans. Electron Devices*, **64**, 796 (2017).
4. G. Tang, A. M. H. Kwan, R. K. Y. Wong, J. Lei, R. Y. Su, F. W. Yao, Y. M. Lin, J. L. Yu, T. Tsai, H. C. Tuan, A. Kalnitsky, and K. J. Chen, *IEEE Electron Dev. Lett.*, **38**, 1282 (2017).
5. T. L. Duan, J. S. Pan, and D. S. Ang, *ECS Journal of Solid State Science and Technology*, **5**, P514 (2016).
6. Y. Dong, R. M. Feenstra, and J. E. Northrup, *Appl. Phys. Lett.*, **89**, 171920 (2006).
7. S. Liu, S. Yang, Z. Tang, Q. Jiang, C. Liu, M. Wang, B. Shen, and K. J. Chen, *Appl. Phys. Lett.*, **106**, 051605 (2015).
8. Z. H. Liu, G. I. Ng, H. Zhou, S. Arulkumaran, and Y. K. T. Maung, *Appl. Phys. Lett.*, **98**, 113506 (2011).
9. Y. Hao, L. Yang, X. H. Ma, J. g. Ma, M. y. Cao, C. y. Pan, C. Wang, and J. c. Zhang, *IEEE Electron Dev. Lett.*, **32**, 626 (2011).
10. Z. H. Liu, G. I. Ng, S. Arulkumaran, Y. K. T. Maung, K. L. Teo, S. C. Foo, and V. Sahmuganathan, *Appl. Phys. Lett.*, **95**, 223501 (2009).
11. S. Huang, S. Yang, J. Roberts, and K. J. Chen, *Physica Status Solidi*, **9**, 923 (2012).
12. T. D. Huang, X. L. Zhu, K. M. Wong, and K. M. Lau, *IEEE Electron Dev. Lett.*, **33**, 212 (2012).
13. M. R. Coan, J. H. Woo, D. Johnson, I. R. Gatabi, and H. R. Harris, *J. Appl. Phys.*, **112**, 024508 (2012).
14. X. Qin and R. M. Wallace, *Appl. Phys. Lett.*, **107**, 081608 (2015).
15. X. Qin, H. Dong, J. Kim, and R. M. Wallace, *Appl. Phys. Lett.*, **105**, 141604 (2014).
16. T. L. Duan, J. S. Pan, and D. S. Ang, *Appl. Phys. Lett.*, **102**, 201604 (2013).
17. C. L. Hinkle, A. M. Sonnet, E. M. Vogel, S. McDonnell, G. J. Hughes, M. Milojevic, B. Lee, F. S. Aguirre-Tostado, K. J. Choi, H. C. Kim, J. Kim, and R. M. Wallace, *Appl. Phys. Lett.*, **92**, 071901 (2008).
18. H. D. Lee, T. Feng, L. Yu, D. Mastrogiovanni, A. Wan, T. Gustafsson, and E. Garfunkel, *Appl. Phys. Lett.*, **94**, 222108 (2009).
19. E. J. Tarsa, B. Heying, X. H. Wu, P. Fini, S. P. DenBaars, and J. S. Speck, *J. Appl. Phys.*, **82**, 5472 (1997).
20. E. D. Readinger, S. D. Wolter, D. L. Waltemyer, J. M. Delucca, S. E. Mohney, B. I. Prenitzer, L. A. Giannuzzi, and R. J. Molnar, *J. Electron. Mater.*, **28**, 257 (1999).
21. Y. Shu, T. Zhikai, W. King-Yuen, L. Yu-Syuan, L. Yunyou, H. Sen, and K. J. Chen, *presented at the Electron Devices Meeting (IEDM)*, 2013 IEEE International, 2013 (unpublished).
22. H. S. Craft, A. L. Rice, R. Collazo, Z. Sitar, and J. P. Maria, *Appl. Phys. Lett.*, **98**, 082110 (2011).
23. J. A. Dean, *Lange's handbook of chemistry*, 15th ed. McGraw-Hill, New York, 2005, (2005).
24. S. Ruvimov, Z. Liliental-Weber, J. Washburn, D. Qiao, S. S. Lau, and P. K. Chu, *Appl. Phys. Lett.*, **73**, 2582 (1998).
25. R. Garcia-Diaz, G. H. Cocoletzi, and N. Takeuchi, *J. Cryst. Growth*, **312**, 2419 (2010).
26. V. M. Bermudez, *Surf. Sci. Rep.*, **72**, 147 (2017).
27. K. T. Jacob and G. Rajitha, *J. Cryst. Growth*, **311**, 3806 (2009).
28. M. S. Miao, J. R. Weber, and C. G. Van de Walle, *J. Appl. Phys.*, **107**, 123713 (2010).
29. Y. Dong, R. M. Feenstra, and J. E. Northrup, *J. Vac. Sci. & Technol. B*, **24**, 2080 (2006).
30. T. L. Duan, L. Pan, Z. Zhang, E. S. Tok, and J. S. Pan, *Surface & Interface Analysis*, (2017).
31. H. W. Jang, K. W. Ihm, T. H. Kang, J. H. Lee, and J. L. Lee, *Phys. Status Solidi B*, **240**, 451 (2003).
32. T. L. Tansley and R. J. Egan, *Phys Rev B Condens Matter*, **45**, 10942 (1992).